


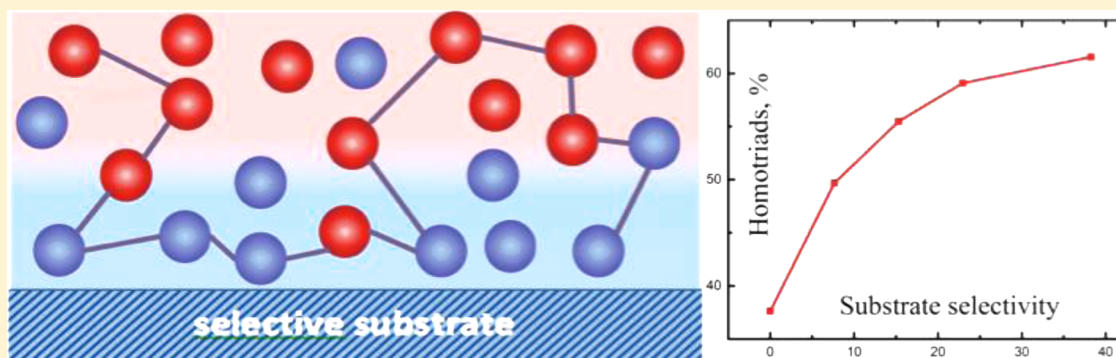
Copolymerization on Selective Substrates: Experimental Test and Computer Simulations

Elena Yu. Kozhunova,^{*,†} Alexey A. Gavrilov,[†] Mikhail Yu. Zaremski,[‡] and Alexander V. Chertovich[†]

[†]Faculty of Physics, M.V. Lomonosov Moscow State University, Leninskiye Gory 1-2, Moscow, Russia 119991

[‡]Faculty of Chemistry, M.V. Lomonosov Moscow State University, Leninskiye Gory 1-3, Moscow, Russia 119991

 Supporting Information



ABSTRACT: We explore the influence of a selective substrate on the composition and sequence statistics during the free radical copolymerization. In particular, we study the radical copolymerization of styrene and acrylic acid in bulk and in silica pores of different sizes. We show that the substrate affects both polymer composition and sequence statistics. We use dissipative particle dynamics simulations to study the polymerization process in detail, trying to pinpoint the parameters responsible for the observed differences in the polymer chain composition and sequences. The magnitude of the observed effect depends on the fraction of adsorbed monomer units, which cannot be described in the framework of the copolymerization theories based on the terminal unit model.

INTRODUCTION

Copolymerization is a versatile synthetic tool for controlling the polymer composition and, therefore, chemical, biological, and physical properties of polymer materials and single macromolecules. In addition to the overall composition, several important properties of the resulting copolymers are provided by local sequence statistics (i.e., chain blockiness and other monomer–monomer correlations along the sequence). That is, the monomer sequence itself controls the macromolecular self-assembly and even some macroscopic properties. For example, properties such as conductivity, elasticity, or biodegradability can be tuned by changing the copolymer sequence. The behavior of polymers in solutions also depends strongly on their monomer sequences. Thus, sequence regulation may enable more effective control of structure-properties relations in novel polymer materials.¹

There are several relevant kinetic models of the copolymerization process, where the reactivity of a growing macroradical depends only on its sequence. The simplest is the terminal model, where it is assumed that the chain propagation reaction is controlled only by the terminal unit of a growing polymer chain. In more advanced penultimate models, it is assumed that both terminal and penultimate units of the growing polymer chain affect its characteristics. Other models

include the influence of side-reactions (such as depropagation, monomer partitioning, and various forms of complex formation); see papers in refs 2 and 3 for a comprehensive review. These models are mainly focused on the sequence statistics and averaged properties, rather than a description of the reaction kinetics coupled with the local surroundings of growing chains.

The other way to control macromolecular self-assembly is the polymerization-induced phase separation, in short PIPS, which is now one of the most promising techniques for novel polymer and composite materials synthesis.⁴ There are several examples of such approach in the recent literature, including the synthesis of new ion-exchange^{5,6} and porous⁷ polymer materials and preparation of cross-linked glasslike microheterogeneous thermosets.⁸ Usually, polymerization starts with large presynthesized precursors, and only one component is polymerized. That is, classical PIPS is relatively well-studied only as homopolymerization modification of polymer blends. It seems encouraging to integrate copolymerization and PIPS in one reactive media. The phase separation could occur during

Received: February 6, 2017

Revised: March 20, 2017

Published: March 22, 2017



the copolymerization process as soon as the growing polymer segments become incompatible. This could be done if a certain degree of blockiness is present, and the blocks formed by different monomers are at least partly immiscible; growing multiblock copolymers could undergo microphase separation in the reaction volume. Obtaining structured, probably long-range ordered polymer matter directly in a reaction volume is an intriguing prospect. We can formulate here two main preliminary requirements for PIPS during the bulk copolymerization: (i) partial incompatibility of the monomer species, characterized by the Flory–Huggins χ parameter, and (ii) multiblock structure of the growing sequence, characterized by the mean block length n . Development of a certain χn value during the polymerization could result in the system undergoing microphase separation.

Simultaneous copolymerization and self-organization of partly immiscible components could provide many opportunities for microstructuring design, especially in the case of thin films. Nowadays, the general trend in both research and development is to work on the micro- and nanoscale, thus understanding the copolymerization processes taking place in thin films several nanometers thick is important for such applications as polymerization in ultraporous materials and clays, lithography channels, in the presence of carbon nanotubes and sheets, or different ultrathin coatings.

From the experimental point of view, some ideas of copolymerization coupled with spatial segregation are realized in the implementation of the selective sorption effect—so-called bootstrap effect.^{9,10} Bootstrap effect is observed when growing polymer chain affects its own environment, which changes the concentration of monomers near the growing polymer chains compared to the system-averaged concentrations. Most frequently this happens during solution copolymerization of mixtures composed of a hydrophobic monomer and a hydrophilic monomer, such as styrene–acrylamide, styrene–methacrylic acid, and styrene–acrylic acid. In that case, the hydrophilic monomer is specifically sorbed on the growing polymer chains, thereby changing the local concentration of the monomer around the active center. The longer the hydrophilic chain precursor is used, the more pronounced the effect.¹¹ Such copolymerization could serve as an example of systems that cannot be correctly described by the simple kinetic copolymerization theories because these theories do not consider possible heterogeneities in the reaction media.

In these circumstances, the aid can come from computer simulation experiments. Nowadays, computer simulations methodology is rapidly growing, as well as computational resources. The studies and characterization of the properties of new materials have largely benefited from *in silico* experiments.^{12,13} The most relevant to our discussion are works from Genzer's group, studying different types of surface and bulk-initiated homopolymerization,^{14,15} and “grafting through” copolymerization on one-dimensional (1D) and two-dimensional (2D) substrates.^{16,17} Also Starovoitova et al. studied the copolymerization of a single molecule near a selectively adsorbing surface and found the formation of gradient copolymers.¹⁸ In our previous works,^{19,20} we performed three-dimensional (3D) computer simulations of PIPS occurring during polycondensation. In the present work, we want to move our focus to the radical copolymerization reaction because of its larger usability and broad applicability.

There are two levers that contribute to the phase separation during radical copolymerization. First is a high value of χ , which

provides components incompatibility. Second, the reactivity ratios r_1 and r_2 , which control the sequence statistics, should be significantly large. Unfortunately, these factors usually work in opposite directions, as high χ value means that the monomers have different chemical nature and reactivity ratios usually far below unity. On the contrary, both reactivity ratios r_1 and r_2 could be rather large only in the case when the monomers have similar chemical nature and, therefore, a low χ value. That is, typical free radical copolymerization gives the reaction product as a statistical copolymer with $n < 2.0$, resulting in homogeneous spatial structure. This is the effect of the donor–acceptor mechanism of the chain propagation resulting in alternating polymer sequences when both $r_1, r_2 < 1.0$. Therefore, there is almost no hope to obtain PIPS in common conditions, and one should consider some strong additional factors that can push up χ or/and r_1 and r_2 . Such additional factor could be the introduction of system heterogeneity. We already mentioned the bootstrap effect hereinbefore, which is a nice example of spatial heterogeneity developed during the copolymerization. But much more opportunities could be provided by strong and stationary inhomogeneity like selective substrates because it could dramatically change the local species concentrations and thus would change the chain blockiness. This research is focused on the copolymerization in small pores with selective surface, which adds spatial inhomogeneity into the system. We have chosen copolymerization of styrene (S) and acrylic acid (A) for our study because it is known that block copolymers of these chemicals could undergo microphase separation even in the case of rather short blocks.²¹ The carboxylic acids in the A block self-associate strongly through the hydrogen-bond interaction. In addition, the copolymerization of this pair is well-studied in detail,^{22,23} including modern living polymerization schemes, both RAFT^{24,25} and NMP.^{26,27}

The main purpose of this work is to study the copolymer composition and sequence statistics during the free radical copolymerization both in bulk and near a substrate with affinity to one of the reacting monomers because the structure of the polymer chain in the vicinity of the substrate is not obvious. We will try to experimentally assess the chain sequence obtained during the copolymerization of S-A, and use computer simulations for more detailed analysis. We will show that the substrate affects both the polymer composition and the sequence statistics.

METHODOLOGY

Materials. All monomers, styrene (S), acrylic acid (A) (Aldrich), were distilled under reduced pressure prior to use. The initiator, benzoyl peroxide (BPO), was recrystallized from ethanol. The substrate, silica “Silochrome S-80” (Si–OH-40) (Reachem), with specific surface area of 80 m²/g and 40 nm pore size, was washed three times in 10% HCl and then in distilled water until neutral pH was obtained. The suspension was centrifuged and sediment fraction with the particle size of 0.15–0.5 mm was dried under vacuum at 110 °C and 10^{−2} mm Hg for 24 h. Silica “Silicagel L100/160” (Si–OH-8) (Lachema), with specific surface area of 310 m²/g and 8 nm pore size, was purified by the same procedure.

Bulk Copolymerization. Copolymerization mixtures were prepared as follows: initiator benzoyl peroxide was weighted into a 7 mL vial ($c = 1 \times 10^{-2}$ M) followed by addition of styrene and acrylic monomers in mol % 90:10, 80:20, and 50:50. The reaction mixtures were degassed by several freeze–thaw cycles in a vacuum down to 10^{−2} mm Hg and sealed off. The samples were placed in thermostat at 80 °C for 15–100 min depending on sample composition so that polymer conversion did not exceed 15%. Obtained copolymers were isolated from the reaction mixture by a lyophilization with dioxane in

vacuum, and a 4-hydroxy-TEMPO inhibitor was added prior to dioxane treatment.

Polymerization in Silica Pores. The procedure was based on polymerization in silicagel pores described in Pavlinec work.²⁸ Special two-neck glass vial was filled with 0.75 mL of mixture containing 1×10^{-2} M solution of benzoyl peroxide in styrene and acrylic acid monomers in mol % 90:10, 80:20, 50:50, and 20:80. The two-neck vial was connected via a flexible vacuum hose with a clip to an evacuated spherical ampule 2 cm in diameter, containing 1 g of dried silica. The reaction mixtures were degassed by several freeze–thaw cycles in a vacuum down to 10^{-2} mm Hg and sealed off. Then the clip to ampule with silica was removed, and the reaction mixture was poured into it. The ampule was sealed off, and its content was thoroughly mixed. The samples looked like powder even when the styrene fraction was 90%. The samples were placed in a thermostat at 80 °C for 10–100 min, depending on sample composition so that monomer conversion did not exceed 15%. After polymerization, the samples were placed in a Soxhlet extractor to remove the absorbed polymer from silica by applying boiling in dioxane for 15–20 cycles; 4-hydroxy-TEMPO inhibitor was added prior to dioxane treatment. Finally, the obtained copolymers were lyophilized with dioxane in vacuum. Using specific surface area of silica and monomer mixture volume, we calculated the approximate thickness of reagents layer near the surface, it could be roughly estimated as 24 monomer units in the case of Si–OH-40 and about 6 in the case of Si–OH-8. The overall pore volume is larger than the volume of the initial monomer solution; a single pore size is also much larger than the size of a monomer the pore filling proceeds in vacuum, so there is no reason that would prevent styrene from entering the pores, presumably meaning that the polymerization proceeds mainly in the pores. Also we assume that the initiator is uniformly distributed in the reaction volume.

Characterization. Copolymer composition was determined by IR spectroscopy with a spectrometer Specord-M80. Samples for the IR spectroscopy were prepared in the form of thin films on fluorite glass from 1% dioxane solution. Chemical composition was calculated using the calibration between absorbance of the band of acrylic acid ($\nu = 1705 \text{ cm}^{-1}$) and styrene ($\nu = 700$ and 1600 cm^{-1}). The results are presented in Table S1 and Figure 2; error bars are indicated according to the standard instrumental error. Typical spectra could be found in Figure S1. ^1H NMR spectra were obtained using Bruker Avance 600 MHz spectrometer at 30 °C. Sample concentration = 1% (g/mL) in CDCl_3 -DMSO- d_6 solvent mixtures, spectral width = 10964.91 Hz, acquisition time = 2.98 s, and spectrum type = DOSY.

Molecular weight distribution of the obtained copolymers was analyzed using GPC-120 PolymerLabs device. The chromatography was employed under 50 °C in mobile phase DMF with LiBr (0.1%). The flow rate was 1.0 mL/min. The samples were separated with a system of two columns PLgel 5 μm MIXED B. The system was calibrated with monodisperse PMMA standards. All obtained copolymers have the similar values of molecular weight in the order of $M \sim 1 \times 10^4$ to 1×10^5 (Figure S2).

Simulation Methodology. Dissipative particle dynamics (DPD) is a simulation of the coarse-grained molecular dynamics adapted to polymers and mapped onto the classical lattice Flory–Huggins theory.^{29–32} It is a well-known method which has been used to simulate properties of a wide range of polymeric systems, such as single chains in solutions,³³ polymer melts,³⁴ and composites.^{35–37} In short, macromolecules are represented in terms of the bead-and-spring model (each coarse-grained bead usually represents a group of atoms), with beads interacting by a conservative force (repulsion) \mathbf{F}_{ij}^c , a bond stretching force (only for connected beads) \mathbf{F}_{ij}^b , a dissipative force (friction) \mathbf{F}_{ij}^d , and a random force (heat generator) \mathbf{F}_{ij}^r . We note here, that the use of soft potentials and original parallel program code allows us to speed up the calculation in 2 orders of magnitude, in comparison with standard MD schemes. We do not provide here a more detailed description and parameters discussion of the standard DPD scheme; it can be found elsewhere.³²

We will study the S-A copolymerization process, so we have two types of monomers, called A (acrylic acid) and S (styrene). As far as we have two types of beads, an additional parameter χ could be

introduced as the interaction parameter between monomers A and S. This is a well-known in polymer theory Flory–Huggins parameter,³⁸ which is directly connected to the soft core repulsion parameter in the

$$\text{DPD conservative force } \mathbf{F}_{ij}^c = \begin{cases} a_{\alpha\beta}(1 - r_{ij}/R_c)r_{ij}/r_{ij}, & r_{ij} \leq R_c \\ 0, & r_{ij} > R_c \end{cases}, \quad a_{\alpha\beta} =$$

$\chi/0.286 + 25$ ($\alpha \neq \beta$), see ref 32. Here R_c is the potential cutoff distance ($R_c = 1.0$); later we will measure all spatial distances in these units. Periodic boundary conditions were applied in all three directions except for the case when we studied copolymerization near a selective substrate, where repulsive impenetrable walls were used in the Z direction instead of periodic boundaries. We assumed strong repulsion between the walls and S-beads, which corresponds to an effective Flory–Huggins-like interaction parameter χ_{eff} effectively mimicking preferential sorption of A-beads. We studied different χ_{eff} and χ parameters, but for the majority of simulations, we fixed the Flory χ -value equal to 0.0 to minimize the number of variable parameters.

The reaction implementation in polymer simulations is more or less common nowadays and several examples can be found in papers.^{39–41} To run polymerization, we will use a scheme similar to that presented in Genzer's paper,¹⁴ with some simplifications described below. First of all, we do not consider the chain transfer and termination reactions. This simplification is reasonable if we study only small conversion values (about 10%), and a small fraction of active ends simultaneously exist in the system representative volume. Second, for simplicity reasons and to reduce the number of simulation parameters, we assumed the initiation process to be immediate (i.e., a certain fraction of random beads set to be active centers at the start of simulations) and set the reaction radius at $R_0 = 1.0$ (i.e., the same as standard DPD interaction radius R_c). While the reaction radius can affect the resulting copolymers (especially in the case of nonhomogeneous systems), it seems natural to choose it to be equal to the interaction radius R_c , two polymer segments become in contact when they are located closer than R_c , which means that they are able to form a bond between each other. See Figure 1 for the simulated system outlook.

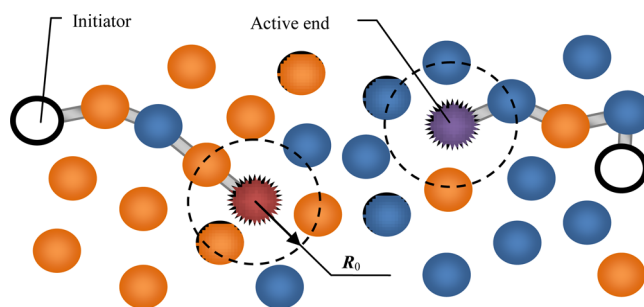


Figure 1. Schematic illustration of the system under study and the reaction scheme.

To model the reaction process, we use a standard Monte Carlo scheme, the reaction procedures run after each τ_0 DPD steps. We set the time interval between reaction steps to be fixed $\tau_0 = 200$ DPD steps. This value is large enough to have local spatial equilibration of the nearest surrounding of each active center. The reaction step consists of the following stages: (1) some active center i is selected randomly. (2) The closest to i monomer bead j (located within the reaction radius) is selected. (3) A random number from $\{0;1\}$ interval is generated, and this number is compared to the chosen reaction probability (reaction activation barrier) between the selected beads i and j : p_{ij} . If the random number is lower than p_{ij} , a new bond between i and j beads is formed and the bead j becomes the new active center of the growing polymer chain instead of i . Otherwise, we go to stage 2 and test the second closest monomer unit.

Stages 2–3 are repeated until we test all beads within the reaction radius R_0 of selected active center i or a bond is formed, afterward we go to the stage 1 and select some other randomly chosen active center. During one reaction step, all active centers (on average) are checked and the quantity of which corresponds to the initiator concentration.

See ref 41 for more details concerning the choice of the parameters for the reaction scheme.

We conducted simulations in a flat box of thickness D with the presence of two walls of the area S (see Figure 3b). That simulation box represents polymerization inside a silica pore with the certain volume/surface ratio. In our simulations, the surface area S was fixed at 256×256 DPD units, while the thickness D varied from 4 to 20 DPD units. This corresponds to the layer thickness from 6 to 30 monomer units, which is comparable with the pore size in our lab experiments. The A-adsorbing surfaces at the bottom and top of the simulation box introduce the external system inhomogeneity.

The full reaction probability matrix is defined by 4 parameters: p_{SS} , p_{AA} , p_{AS} , and p_{SA} (later we will consider $p_{SA} = p_{AS}$ for simplicity reasons). In terms of reactivity ratios, we have $r_A = p_{AA}/p_{AS}$ and $r_S = p_{SS}/p_{SA}$. In accordance with the work,²² we set the reactivity ratios to be $r_A = 0.13$ and $r_S = 0.38$ for polymerization in bulk. We note here that several different reactivity ratios for S-A system can be found in the literature, and the values depend strongly on the solvent, temperature, initiator type, and/or mechanism of living process. For instance, in the work⁴² NMP copolymerization of S-A in dioxane was studied and the reactivity ratios were found to be equal to $r_A = 0.27$ for acrylic acid and $r_S = 0.72$ for styrene. In the article,²³ RAFT polymerization in bulk was used and the authors obtained $r_A = 0.082$ and $r_S = 0.21$. We select the parameters from the work²² because in that work the most complete sequence statistics description was presented, including the triads fractions (obtained using ^{13}C NMR), which could readily be compared with the results of computer simulations. Several examples of the copolymer composition-monomer feed curves for a set of r_A and r_S values available in the literature are presented for illustrative purposes in Figure 2. We will show later that the influence of the substrate is observed for any selection of reactivity ratios when both of them are less than or equal to unity.

Thus, we have four variable parameters in our copolymerization simulation scheme: r_A , r_S , χ , and χ_{eff} . To run the simulations, we used original DPD code and performed simulations at the MSU supercomputer facilities (hpc.msu.ru).

RESULTS AND DISCUSSION

Experimental Realization of Styrene-Acrylic Acid Copolymerization. For experimental study of the selective surface influence on radical polymerization, we conducted the synthesis of poly(styrene-co-acrylic acid) using free radical copolymerization in the pores of silica that have an affinity for acrylic acid monomers; to the best of our knowledge, such processes have not been previously described in the literature. We used silica with two different pore sizes, Si-OH-40 and Si-OH-8, where the code number represents the mean pore diameter (in nm). Varying the pore size is the most convenient method to change the volume/surface ratio or the fraction of adsorbed monomer units in the case of selective substrates.

Three series of synthesis were performed under the same conditions: copolymerization in Si-OH-40 pores with four monomer feed ratios, copolymerization in Si-OH-8 pores with three monomer feed ratios, and bulk copolymerization with three monomer feed ratios. Polymerization reaction in each case was stopped when the monomer conversion of the product did not exceed 15% because low monomer conversions allows us to study the changes in both polymer chain sequence and composition without additional effects caused by the exhaustion of available monomers. IR spectra analysis revealed that the copolymers obtained in Si-OH-40 and bulk have approximately the same composition (Figure 2). But copolymerization in smaller pores of Si-OH-8 provided us with a significant shift in the composition of the obtained copolymer. For example, the fraction of acrylic acid F_A in poly(A-co-S) dropped from 35,5 (bulk) to 19,8 (Si-OH-8) mol

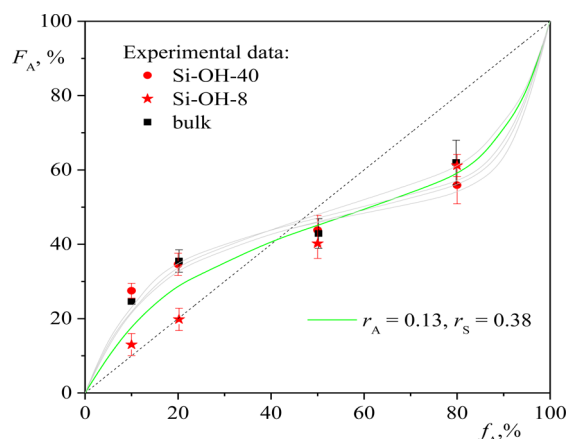


Figure 2. Dependence of the poly(styrene-co-acrylic acid) composition on the initial monomer feed: experimental data are shown as symbols, gray curves represent theoretical curves obtained for different reported reactivity ratios for the S-A reaction, while the green line corresponds to the reactivity ratios from the paper²² which was used in the computer simulations.

%, which is remarkably lower than any previously reported data for the bulk polymerization (see light-gray and green curves in Figure 2, which correspond to different theoretical curves from the literature data¹¹). Note that this downshift is in good agreement with the simulation results (see below). The possible explanation could be the following: A units can adsorb onto the pore surface, which results in the formation of a dense A-layer on the substrate and gives us an S-rich area in the volume. Since most of the chain propagation effects occur in the pore volume, the possibility to form bond between an active end and an S-monomer increases, which results in the observed downshift for the acrylic acid composition F_A . See a detailed discussion below in the computer simulations Results section.

Computer simulation data showed that during copolymerization near selective substrates the triad composition of the polymer chains varies remarkably depending on the type of substrate and its ability to absorb certain monomers, even in the case when the polymer composition changes only slightly. To prove those results experimentally, it was necessary to determine the triad composition of the synthesized copolymers. The NMR method may provide²² an insight into the polymer chain structure which can be performed by means of studying specific resonance peaks for the triad structure analysis. In our research, ^1H NMR spectra were obtained for synthesized samples and two series of spectra were compared—bulk copolymers and Si-OH-40 copolymers. As an example, Figure S3 shows a set of spectra for the polymers synthesized in the pores of Si-OH-40, indicating the most characteristic resonance peaks.

Careful analysis of the spectra for the samples with the same 20:80 A:S feed composition (Figure S4) showed that the shape of obtained NMR peaks varies slightly for Si-OH-40 and bulk cases, which may indicate the difference in the triad composition of the polymer chains. For example, triangular styrene phenyl ring peak was fitted by three Gaussian peaks presumably corresponds to three styrene-centered triads SSS, SSA, and ASA. It was found that the assumed SSS triad central peak increases in the case of the hydrophilic surface compared to that peak in bulk. This observation is in agreement with our computer simulation results and will be explained below. Unfortunately, the NMR peak splits occur to be too small to

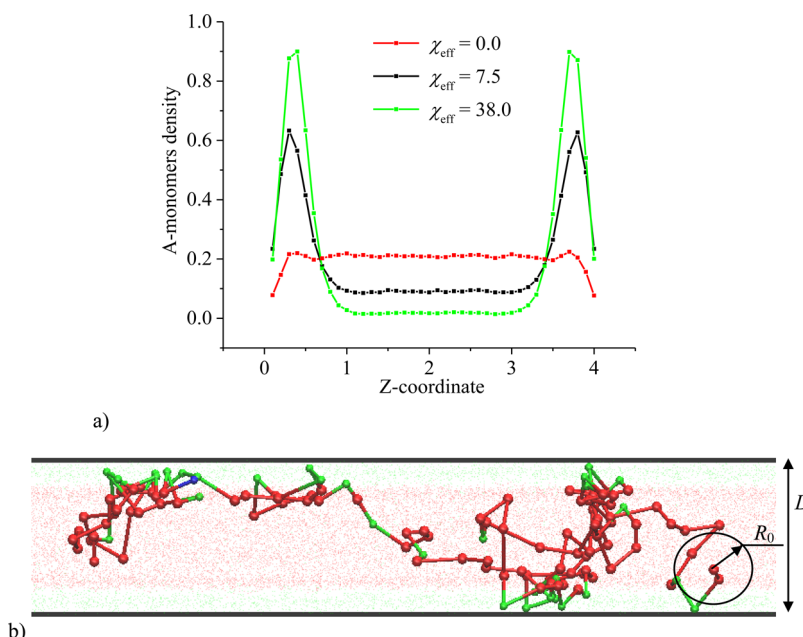


Figure 3. (a) Monomer density profiles at different χ_{eff} values normalized by the average system density; (b) visualization of a single chain between two surfaces with preferential sorption of A beads (green), S beads are red, and the initiator is blue, and nonpolymerized monomers are semitransparent (small dots), while one chosen polymer chain is opaque, $\chi_{\text{eff}} = 30$.

analyze the triads composition in a quantitative manner, so we performed only a qualitative comparison here.

Computer Simulation of Styrene-Acrylic Acid Copolymerization. We performed computer simulations for an asymmetric case of minor A-fraction and preferential surface sorption of A-beads to understand the composition of copolymer forming within the silica pores in comparison to the bulk reaction in volume in detail. The monomers density profiles depend on the surface-layer interaction or the “substrate selectivity parameter” χ_{eff} . Profiles distort with the increase of χ_{eff} until almost all A-units relocate close to the adsorbing surface; resulting concentration profiles are presented in Figure 3a. After some initial equilibration, the reaction was initiated by immediate activation of 0.1% fraction of randomly chosen monomer units as active centers, and the ensemble of chains started to grow. At least 786 chains were growing simultaneously in the simulation box (for the smallest pore size with $D = 4$), thus the results were averaged well over many sequences. Similar to the lab experiments, we stopped the polymerization upon achieving 10% conversion corresponding to the average chain length of 100 monomer units, which already gives reasonable errors while calculating the sequence statistics. We would like to note that the spatial species profiles stay almost unchanged during the polymerization process and remain in a form similar to that presented in Figure 3a.

Visualization of a single chain helps to understand the process occurring during the polymerization in a pore (Figure 3b). We can see that green A beads concentrate mainly near surfaces, giving us bigger S-rich area in the middle and that the chain travels through the pore depth back and forward from one substrate to the opposite one. In general, it could be said that the growing polymer chain polymerizes in partly segregated media, fixing its spatial structure.

The main results of our simulations of S-A polymerization inside a pore are presented in Figure 4. Figure 4a gives a copolymer composition F_{AA} versus varied substrate selectivity χ_{eff} and different pore sizes, with fixed $\chi = 0.0$, $r_{\text{A}} = 0.13$, and r_{S}

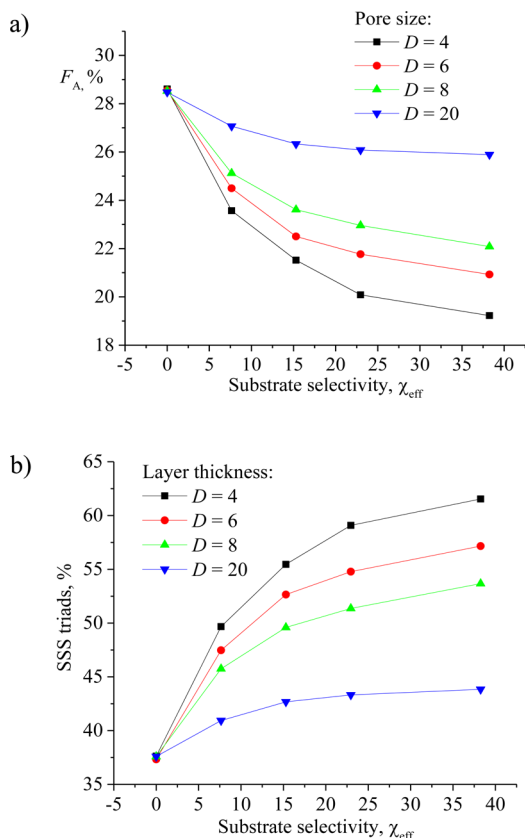


Figure 4. (a) Computer simulation of copolymer composition for fixed monomer feed, 20:80 A:S, depending on the substrate selectivity χ_{eff} . (b) Computer simulation of SSS triad fraction for the same monomer feed depending on the substrate selectivity χ_{eff} .

$= 0.38$. One can see that there is a downshift in the averaged copolymer composition observed upon both pore size decrease and substrate selectivity increase. But the difference is clear and

Table 1. Triad Distributions and Observable Reactivity Ratios of Copolymers Obtained by Polymerization in Bulk and in Pores, f_A is a feed Fraction of Acrylic Acid, F_A is the Fraction of Acrylic Acid in Obtained Copolymer

	AAA (%)	AAS (%)	SAS (%)	SSS (%)	SSA (%)	ASA (%)	F_A (%)	observable reactivity ratios
bulk, $f_A = 11\%$	0.02	2.70	97.28	58.11	36.30	5.59	19.40	$r'_A = 0.13 \pm 0.02$ $r'_S = 0.38 \pm 0.01$
pores, $D = 4$, $\chi_{\text{eff}} = 38$, $f_A = 20\%$	0.36	10.57	89.07	61.79	31.63	6.58	19.11	$r'_A = 0.24 \pm 0.01$ $r'_S = 0.90 \pm 0.02$

significant only at small pore sizes and high sorption parameter χ_{eff} . Let us discuss the origin of this downshift. The strong adsorption of A-units dramatically changes the shape of the concentration profiles (see Figure 3), therefore the local concentration of monomer units around the growing chain end significantly differs from the average monomer feed. Inside the pore volume, there is much less A-units in comparison to the average monomer feed, so a growing chain end located in the pore volume is situated in the S-enriched environment. When a growing chain end is located in the dense but very thin layers of adsorbed A-units, it still contacts with the S-enriched pore volume because the thickness of the layers is comparable to the monomer size. Thus, the surrounding of an active growing chain end does not correspond to the system average composition, resulting in the decrease of A-fraction in polymerized sequences. We believe that the same mechanism is valid also for the experimental setup, since strong interaction between acrylic acid and Si–OH substrate probably helps to form a thin and dense layer of adsorbed monomer units.

In addition to the polymer composition, we studied the statistical properties of obtained sequences, namely triad distributions. This is more “local” attribute of copolymer sequence in contrast to “system averaged” copolymer composition. Figure 4b presents the SSS-triad fraction (AAA-triads have a similar behavior but strongly fluctuate because of the small statistics for the minor A-component) at different pore size and different sorption value. There is a considerable increase in SSS-triad fraction for all systems under study, indicating that the blockiness of the sequences increases. Note that this effect is more pronounced than the average composition discussed previously. See also Figure S5 for computer simulation images of monomer sequences along the obtained polymer chains.

For more convenient assessment of the sequence statistics, we introduce here a special derivative of the monomer units' positions along the polymer chain. Namely, we calculate the “observable” reactivity ratios r' from a direct analysis of the obtained sequences, in addition to preset values $r_A = 0.13$ and $r_S = 0.38$. That is, we can calculate the real probabilities to find two consequential A-units, two consequential S-units, A-unit after S-unit and vice-versa (i.e., p'_{AA} , p'_{SS} , p'_{AS} , and p'_{SA}) by “scanning” along the chains and then directly calculate $r'_A = p'_{AA}/p'_{AS}$ and $r'_S = p'_{SS}/p'_{SA}$. We distinguish these “observable” r'_A and r'_S from the fixed input reaction rate parameters r_A and r_S because they take into account the local surrounding of the growing chain and possible heterogeneities.

Author: We found that the observable reactivity ratios change drastically when the selective substrate is introduced. For the representative case, we simulated bulk polymerization and in-pore polymerization that give the same ratio of acrylic acid in the obtained copolymer, F_A . It could be seen (Table 1) that the observable reactivity ratios for bulk copolymerization are equal to the preset reactivity ratios, but for polymerization near the

selective surfaces the reactivity ratios, and thus blockiness of the chain, increase significantly.

Up to this point, we assumed that the parameter χ , interaction parameter between monomers, was equal to zero. Let us now check the influence of χ on the copolymer composition to see whether that assumption was reasonable. Figure 5 presents the simulated dependence of the copolymer

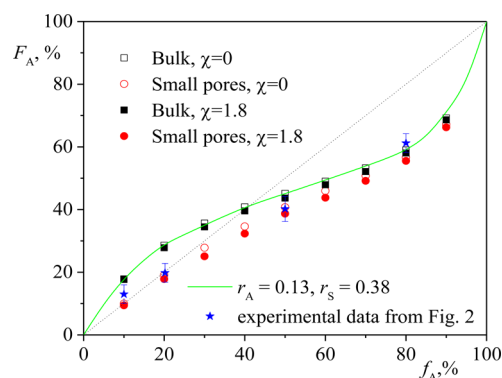


Figure 5. Calculated dependences of F_A on f_A for two sets of χ parameters.

composition, F_A , on the monomer feed, f_A , both in bulk and in small pores ($D = 4$, $\chi_{\text{eff}} = 38$) for $\chi = 0$ and $\chi = 1.8$. It could be seen that F_A is almost independent of χ variation. Even for very high parameter $\chi = 1.8$, the difference is comparable with the error bar (which is the same size as the symbol size). We note here that according to the work,²¹ a reasonable estimation of χ value for styrene and acrylic acid pair is about 0.2. Detailed investigation of the influence of χ on the copolymer sequences (in bulk) could be found in a separate work.⁴¹ In addition, experimental data from the synthesis in small pores are given in Figure 5 and there is very good, although not excellent, agreement with the simulations results; one should note that in order to obtain quantitatively similar to experiments results in simulations, it is necessary to calibrate the coarse-grained reaction model using more sophisticated force-fields (or even quantum chemistry calculations) in order to properly couple the interaction and reaction characteristic lengths to each other. Therefore, when comparing the experimental and simulation results, we can only talk about general qualitative trends. We also note here that the effect of the substrate influence on the composition is well-pronounced only for minor fractions of adsorbing A-units. The maximum deviation from the bulk values is observed at around 20% acrylic acid in the monomer feed.

Computer Simulation of Generalized Case with $r_A = r_B = 1.0$. It was shown in the previous parts that sufficiently small pores and strong preferential interactions between monomers and substrate could affect the composition of obtained copolymer. Now we will check if this result is correct for other sets of reactivity ratios using a very model symmetric

reaction with $r_A = r_B = 1.0$ and $\chi = 0$, corresponding to absolutely random AB-copolymer with mean block length $n = 2.0$ at 50:50 feed composition and homogeneous bulk structure. The pore size was again fixed to its minimum value $D = 4$, and the substrate selectivity was fixed at its highest $\chi_{\text{eff}} = 38$. We calculated the copolymer composition curve in bulk and inside pores and corresponding “observable” reactivity ratios r'_A and r'_B ; the results are presented in Figure 6.

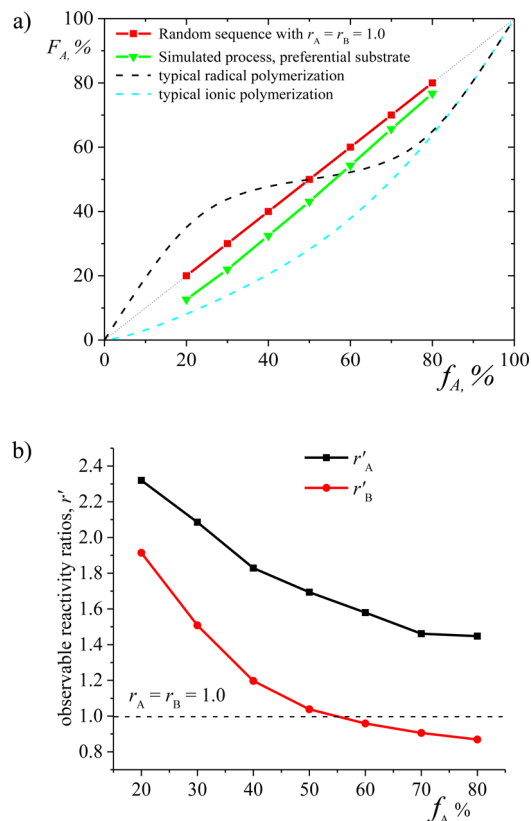


Figure 6. (a) Simulated copolymer composition–monomer feed curves for reaction taking place in bulk and small pores, $r_A = r_B = 1.0$, $D = 4$, $\chi_{\text{eff}} = 38$. Dashed curves represent typical behavior for radical and ionic copolymerization and are drawn as a guide to the eye. (b) Dependence of the observable r'_A and r'_B on the monomer feed composition. The dashed horizontal line in (b) represents the case of “truly” random copolymerization with $r_A = r_B = 1.0$.

Looking at these results one can conclude that the selective substrate can change the copolymerization behavior even for this model case, moving down the composition–feed curve, see Figure 6a; this shift is larger for minor fractions of adsorbing A units. The changes in sequence statistics are more pronounced if we check the absolute values of “observable” reactivity ratios, see Figure 6b. The polymerization proceeds in already partly segregated system, due to the surface influence, which leads to an increase in the sequence blockiness and, thus, to changes in the observable reaction rate. One can see that both observable values r'_A and r'_B for 50% feed composition and less overcome the threshold $r = 1.0$ (corresponding to the mean block length of $n = 2.0$). With the increase of the A feed ratio, the influence of the surface on the overall monomer composition weakens because only certain amount of A units could adsorb on the surface and the concentration profile changes upon introduction of the selective surfaces become less pronounced.

SUMMARY AND CONCLUSIONS

To summarize, our study shows that the selective substrate affects both copolymer composition and sequence blockiness during free-radical copolymerization. This effect is more pronounced when the polymerization occurs in small pores or thin layers, where the ratio between the substrate surface and bulk volume is high. The reason is the partial spatial separation of monomer units, due to selective adsorption to the substrate, leading to changes in the local concentration of monomer units around the growing chain end. In addition to the shift in the polymer composition, the sequence statistics undergoes even more pronounced changes. Namely, the chain blockiness increases, which can be detected via comparison of the triad fractions or by calculating the observable reactivity ratios.

We have shown that the observed effects are present in other systems in which the copolymerization takes place near a substrate with preferential adsorption of one type of monomers; namely, we tested the case of both reactivity ratios being equal to 1.0. The substrate influence is more pronounced when the substrate attracts monomers that are in smaller fraction in the monomer feed mixture because in that case the volume concentration of that monomer decreases significantly.

Another essential conclusion is that the effect of selective substrate cannot be described by simple copolymerization theories. That is, the standard terminal models and even complicated penultimate and pen-penultimate models do not consider possible heterogeneity of the reaction media. The simplest contradiction can be clearly seen from Figure 6b, where observable reactivity ratios depend strongly on the monomer feed, while this cannot be true for existing theories based on the terminal unit model.

ASSOCIATED CONTENT

Supporting Information

The Supporting Information is available free of charge on the ACS Publications website at DOI: 10.1021/acs.langmuir.7b00406.

Chemical composition of the copolymers, IR spectroscopy data, GPC data, ^1H NMR spectra and its analysis, and additional computer simulations results (PDF)

AUTHOR INFORMATION

Corresponding Author

*E-mail: kozhunova@poly.phys.msu.ru.

ORCID

Elena Yu. Kozhunova: 0000-0003-2062-004X

Notes

The authors declare no competing financial interest.

ACKNOWLEDGMENTS

We appreciate the financial support from the Russian Science Foundation (Project no. 14-13-00683). The authors thank Moscow State University Supercomputer Center (hpc.msu.ru) for providing the computational resources and Professor Vladimir Polshakov and the Center for Magnetic Tomography & Spectroscopy for ^1H NMR spectroscopy measurements.

REFERENCES

- (1) Lutz, J.-F.; Ouchi, M.; Liu, D. R.; Sawamoto, M. Sequence-Controlled Polymers. *Science* **2013**, *341* (6146), 1238149–1238149.

- (2) Coote, M. L.; Davis, T. P. The Mechanism of the Propagation Step in Free-Radical Copolymerisation. *Prog. Polym. Sci.* **1999**, *24* (9), 1217–1251.
- (3) Coote, M. L.; Davis, T. P.; Klumperman, B.; Monteiro, M. J. A Mechanistic Perspective on Solvent Effects in Free-Radical Copolymerization. *J. Macromol. Sci., Polym. Rev.* **1998**, *38* (4), 567–593.
- (4) Inoue, T. Reaction-Induced Phase Decomposition in Polymer Blends. *Prog. Polym. Sci.* **1995**, *20* (1), 119–153.
- (5) McIntosh, L. D.; Schulze, M. W.; Irwin, M. T.; Hillmyer, M. A.; Lodge, T. P. Evolution of Morphology, Modulus, and Conductivity in Polymer Electrolytes Prepared via Polymerization-Induced Phase Separation. *Macromolecules* **2015**, *48* (5), 1418–1428.
- (6) Chopade, S. A.; So, S.; Hillmyer, M. A.; Lodge, T. P. Anhydrous Proton Conducting Polymer Electrolyte Membranes via Polymerization-Induced Microphase Separation. *ACS Appl. Mater. Interfaces* **2016**, *8* (9), 6200–6210.
- (7) Oh, J.; Seo, M. Photoinitiated Polymerization-Induced Microphase Separation for the Preparation of Nanoporous Polymer Films. *ACS Macro Lett.* **2015**, *4* (11), 1244–1248.
- (8) Liu, Y. Polymerization-Induced Phase Separation and Resulting Thermomechanical Properties of Thermosetting/reactive Nonlinear Polymer Blends: A Review. *J. Appl. Polym. Sci.* **2013**, *127*, 3279–3292.
- (9) Harwood, H. J. Structures and Compositions of Copolymers. *Makromol. Chem., Macromol. Symp.* **1987**, *10–11* (1), 331–354.
- (10) Semchikov, Y. D. Preferential Sorption of Monomers and Molecular Weight Effects in Radical Copolymerization. *Macromol. Symp.* **1996**, *111* (1), 317–328.
- (11) Borisova, O. V.; Zaremski, M. Y.; Borisov, O. V.; Billon, L. The Well-Defined Bootstrap Effect in the Macroinitiator-Mediated Pseudoliving Radical Copolymerization of Styrene and Acrylic Acid. *Polym. Sci., Ser. B* **2013**, *55* (11–12), 573–576.
- (12) Liu, A. J.; Grest, G. S.; Marchetti, M. C.; Grason, G. M.; Robbins, M. O.; Fredrickson, G. H.; Rubinstein, M.; Olvera de la Cruz, M. Opportunities in Theoretical and Computational Polymeric Materials and Soft Matter. *Soft Matter* **2015**, *11*, 2326–2332.
- (13) Potestio, R.; Peter, C.; Kremer, K. Computer Simulations of Soft Matter: Linking the Scales. *Entropy* **2014**, *16*, 4199–4245.
- (14) Genzer, J. In Silico Polymerization: Computer Simulation of Controlled Radical Polymerization in Bulk and on Flat Surfaces. *Macromolecules* **2006**, *39* (20), 7157–7169.
- (15) Turgman-Cohen, S.; Genzer, J. Simultaneous Bulk- and Surface-Initiated Controlled Radical Polymerization from Planar Substrates. *J. Am. Chem. Soc.* **2011**, *133* (44), 17567–17569.
- (16) Datta, P.; Genzer, J. Computer Simulation of Template Polymerization Using a Controlled Reaction Scheme. *Macromolecules* **2013**, *46* (6), 2474–2484.
- (17) Datta, P.; Genzer, J. Grafting Through Polymerization Involving Surface-Bound Monomers. *J. Polym. Sci., Part A: Polym. Chem.* **2016**, *54* (2), 263–274.
- (18) Starovoitova, N. Y.; Berezkin, A. V.; Kriksin, Y. A.; Gallyamova, O. V.; Khalatur, P. G.; Khokhlov, A. R. Modeling of Radical Copolymerization near a Selectively Adsorbing Surface: Design of Gradient Copolymers with Long-Range Correlations. *Macromolecules* **2005**, *38* (6), 2419–2430.
- (19) Gavrilov, A. A.; Guseva, D. V.; Kudryavtsev, Y. V.; Khalatur, P. G.; Chertovich, A. V. Simulation of Phase Separation in Melts of Reacting Multiblock Copolymers. *Polym. Sci., Ser. A* **2011**, *53* (12), 1207–1216.
- (20) Gavrilov, A. A.; Chertovich, A. V. Self-Assembly in Thin Films during Copolymerization on Patterned Surfaces. *Macromolecules* **2013**, *46* (11), 4684–4690.
- (21) Cheng, J.; Lawson, R. A.; Yeh, W.-M.; Jarnagin, N. D.; Peters, A.; Tolbert, L. M.; Henderson, C. L. Directed Self-Assembly of Poly(styrene)-Block-Poly(acrylic Acid) Copolymers for Sub-20nm Pitch Patterning; Tong, W. M., Ed.; *International Society for Optics and Photonics*, 2012; pp 83232R-1–83232R-8.
- (22) Wang, S.; Poehlein, G. W. Investigation of the Sequence Distribution of Bulk and Emulsion Styrene–acrylic Acid Copolymers by ¹H- and ¹³C-NMR. *J. Appl. Polym. Sci.* **1993**, *49* (6), 991–1001.
- (23) Harrisson, S.; Ercole, F.; Muir, B. W. Living Spontaneous Gradient Copolymers of Acrylic Acid and Styrene: One-Pot Synthesis of pH-Responsive Amphiphiles. *Polym. Chem.* **2010**, *1* (3), 326–332.
- (24) Llauro, M.-F.; Loiseau, J.; Boisson, F.; Delolme, F.; Ladavière, C.; Claverie, J. Unexpected End-Groups of Poly(acrylic Acid) Prepared by RAFT Polymerization. *J. Polym. Sci., Part A: Polym. Chem.* **2004**, *42* (21), 5439–5462.
- (25) Vishnevetskii, D. V.; Plutalova, A. V.; Yulusov, V. V.; Zotova, O. S.; Chernikova, E. V.; Zaitsev, S. D. Controlled Radical Copolymerization of Styrene with Acrylic Acid and tert-Butyl Acrylate under Conditions of Reversible Addition–Fragmentation Chain Transfer: Control of the Chain Microstructure. *Polym. Sci., Ser. B* **2015**, *57* (3), 197–206.
- (26) Lefay, C.; Charleux, B.; Save, M.; Chassenieux, C.; Guerret, O.; Magnet, S. Amphiphilic Gradient Poly(styrene-Co-Acrylic Acid) Copolymer Prepared via Nitroxide-Mediated Solution Polymerization. Synthesis, Characterization in Aqueous Solution and Evaluation as Emulsion Polymerization Stabilizer. *Polymer* **2006**, *47* (6), 1935–1945.
- (27) Moad, G.; Rizzardo, E.; Thang, S. H. Radical Addition–Fragmentation Chemistry and RAFT Polymerization. In *Polymer Science: A Comprehensive Reference, 10 Volume Set*; **2012**; Vol. 3, pp 181–226 DOI: 10.1016/B978-0-444-53349-4.00066-2.
- (28) Pavlinec, J. Styrene Polymerization in Silica Gel Porous Grains. *Eur. Polym. J.* **1992**, *28* (7), 799–802.
- (29) Hoogerbrugge, P. J.; Koelman, J. M. V. A. Simulating Microscopic Hydrodynamic Phenomena with Dissipative Particle Dynamics. *Europhys. Lett.* **1992**, *19* (3), 155–160.
- (30) Schlijper, A. G.; Hoogerbrugge, P. J.; Manke, C. W. Computer Simulation of Dilute Polymer Solutions with the Dissipative Particle Dynamics Method. *J. Rheol. (Melville, NY, U. S.)* **1995**, *39* (3), 567–579.
- (31) Español, P.; Warren, P. Statistical Mechanics of Dissipative Particle Dynamics. *Europhys. Lett.* **1995**, *30* (4), 191–196.
- (32) Groot, R. D.; Warren, P. B. Dissipative Particle Dynamics: Bridging the Gap between Atomistic and Mesoscopic Simulation. *J. Chem. Phys.* **1997**, *107* (11), 4423–4435.
- (33) Guo, J.; Liang, H.; Wang, Z.-G. Coil-to-Globule Transition by Dissipative Particle Dynamics Simulation. *J. Chem. Phys.* **2011**, *134* (24), 244904.
- (34) Gavrilov, A. A.; Kudryavtsev, Y. V.; Chertovich, A. V. Phase Diagrams of Block Copolymer Melts by Dissipative Particle Dynamics Simulations. *J. Chem. Phys.* **2013**, *139* (22), 224901.
- (35) Raos, G.; Casalegno, M. Nonequilibrium Simulations of Filled Polymer Networks: Searching for the Origins of Reinforcement and Nonlinearity. *J. Chem. Phys.* **2011**, *134* (5), 054902.
- (36) Gavrilov, A. A.; Chertovich, A. V.; Khalatur, P. G.; Khokhlov, A. R. Study of the Mechanisms of Filler Reinforcement in Elastomer Nanocomposites. *Macromolecules* **2014**, *47* (15), 5400–5408.
- (37) Gavrilov, A. A.; Komarov, P. V.; Khalatur, P. G. Thermal Properties and Topology of Epoxy Networks: A Multiscale Simulation Methodology. *Macromolecules* **2015**, *48* (1), 206–212.
- (38) Grosberg, A. I.; Khokhlov, A. R. *Statistical Physics of Macromolecules*; AIP Press, 1994.
- (39) Berezkin, A. V.; Kudryavtsev, Y. V. Simulation of End-Coupling Reactions at a Polymer–Polymer Interface: The Mechanism of Interfacial Roughness Development. *Macromolecules* **2011**, *44* (1), 112–121.
- (40) Genzer, J.; Khalatur, P. G.; Khokhlov, A. R. Conformation-Dependent Design of Synthetic Functional Copolymers. In *Polymer Science: A Comprehensive Reference, 10 Volume Set*; **2012**; Vol. 6, pp 689–723 DOI: 10.1016/B978-0-444-53349-4.00176-X.
- (41) Gavrilov, A. A.; Chertovich, A. V. Copolymerization of Partly Incompatible Monomers: An Insight from Computer Simulations. *Macromolecules*, submitted for publication, 2017.
- (42) Couvreur, L.; Charleux, B.; Guerret, O.; Magnet, S. Direct Synthesis of Controlled Poly(styrene-Co-Acrylic Acid)s of Various Compositions by Nitroxide-Mediated Random Copolymerization. *Macromol. Chem. Phys.* **2003**, *204* (17), 2055–2063.